

Seismic Collapse Analysis For Xiaoyudong Bridge

Axial-Shear-Flexural Interaction



Qi-Wu Fan, Yong-Jiu Qian and Zhen-Xing Feng

Southwest Jiaotong University, the school of civil engineering, Chengdu, China

SUMMARY:

Based on post-earthquake damage assessment and site fault investigation of Xiaoyudong Bridge, collapse process can be speculated and the conclusion is made that the bottoms of inclined legs was the vulnerable component subjected to seismic load. In this paper, based on total strain-based hysteretic material considering cyclic crack closing effect, force-based and displacement-based beam elements are developed to couple shear and flexural responses for axial force variation. In terms of two damage indexes, structural damage state can be represented. The elements are implemented as a user element in ANSYS. The models are used to perform IDA for Xiaoyudong Bridge, and it is shown that the result is compatible with actual damage.

Key words: collapse process, total strain-based hysteretic material, damage index

1. INTRODUCTION

Considerable infrastructures were destroyed in 5.12 Wenchuan Earthquake. Collapse of bridge is an extreme damage state that bridge loses carrying functions completely, and also it will cause huge economic losses and negative social effects. Hence, bridge collapse during earthquake must be prevented. Truss arch bridge has been widely used, especially in western China, in spans ranging from 25m to 75m due to its advantages, such as light quality, integrality, convenience for construction and low cost. Xiaoyudong Bridge is a typical truss arch bridge, and suffered collapse damage during Wenchuan Earthquake. In this paper bridge collapse process and mechanisms have been speculated and deduced. Based on total strain-based hysteretic material considering cyclic crack closing effect, the forced-based and displacement-based beam elements are developed to simulate collapse process and damage state of the bridge coupled axial-shear-flexural interaction.

2. DAMAGE OBSERVATION AND POSSIBLE MECHANISMS OF COLLAPSE

Xiaoyudong Bridge crossing Jianjiang River plays an important role in transportation networks connecting Pengzhou and Longmenshan Town. The bridge is a 187m long, 12m wide, 4 spans, rigid-frame arch bridge which is built in 1998, and each span of the bridge is consisted of 5 ribs with a rise of 5m.

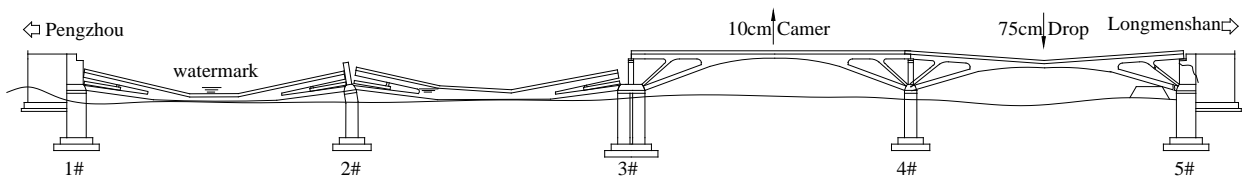


Fig.1 Diagram of post-earthquake situation of Xiaoyudong Bridge



Fig.2 Photo of post-earthquake situation of Xiaoyudong Bridge

2.1. Seismic Damage Observation and Analysis

The Wenchuan Earthquake, which occurred in Sichuan Province, had a magnitude of 8.0 by CEA (China Earthquake Administration). Due to the earthquake, two obvious surface fault displacements occurred around Xiaoyudong bridge site closed to the epicenter. After earthquake, two spans collapsed completely, while two spans on the other side have an significant vertical displacement. The post-earthquake situation of Xiaoyudong Bridge is shown in Fig.1 and Fig.2. According to field surveys after earthquake, there are obvious signs of impact on Abutment 2 and a large number of fractures occurred on the concrete around it. For Span 1, the longitudinal displacement is up to 38cm, and girders fell off Abutment 1. Consequently the arch legs and inclined legs could not support the weight of the bridge so that span 1 collapsed. For Pire 2, the balance of horizontal force came from the legs of both Span 1 and Span 2 at the same time. After the loss of balance due to the drop of Span 1, about 9° tilt towards Abutment 1 occurred to Pire 2, and this resulted in the drop of Span 2. According to the verification of a witness, Span 1 collapsed firstly, and then did Span 2, But the drop of Span 2 did not cause the continuous slump of Span 3. The structure of Span 3 was largely intact, and no obvious damage was found on the pier and at the foot of the arch. Only local shear cracks can be inspected on the pier, and some cracks, caused by inadequate bending capacity under earthquake action, developed at the foot of the arch, but that was not enough to make the structure collapse. Also, large horizontal dislocation between the pier and the girder occurred, and it was about 0.102m according to field surveys. There were obvious cracks on Abutment 5, and in this area, shearing destruction and buckling destruction happened to arch legs and inclined legs. Vertical bending displacements, caused by earth movement and longitudinal deflection, happened to arch ribs, and it was about 0.753m that Span 4 moved downwards. But the structure was not crashed because of the bracing of river bank revetment created by cobblestones.

2.2. Surface Fault Displacement

Direct reason that induced the failure of Xiaoyudong Bridge is large longitudinal and vertical displacement due to surface faults. Two surface fault displacements occurred around the bridge during earthquake as shown in Fig.3. According to field surveys, at the dyke of Pengzhou nearly 70m upstream of the bridge, about 1.5m vertical offset occurred, with 2.8m lateral movement. The fault crossed the bridge at east side about 300m away, run from east to west and it is basically orthotropic to bridge axis. It is considered as the main fault. And this fault displacement extended downstream along the dyke of Pengzhou and crossed the approaching road at 10m, where along with 0.54m surface uplift, and 50m behind Abutment 1. On the other hand, 0.3m settlement at the right bank, at about 50m upstream of the bridge has been found by Kawashima, and it is assumed to be the secondary fault.

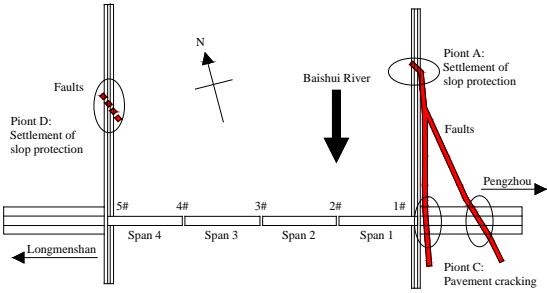


Fig.3 Surface faults around Xiaoyudong Bridge

2.3 Possible Mechanisms of Bridge Collapse

According to field surveys and analysis of damage to the bridge and surface faults, collapse process of the bridge can be speculated, as follows:

- 1) The main fault caused surface rupture zone, and the pavements behind abutment ruptured and uplifted seriously, at the same time Abutment 1 was fractured under the pounding of bridge span, then significant relative displacement in both longitudinal and vertical direction occurred between ribs of Span 1 and Abutment 1, thus Span 1 slid from Abutment 1, after that arch legs and inclined legs could not support the weight of the bridge and cracked, as consequence, Span 1 collapsed.
- 2) After the lost of balance of horizontal force due to the drop of Span 1, Pire 2 tilted towards Abutment 1, at the same time, site liquefaction effect exacerbated the deformation of Pire 2, and this consequently resulted in the collapse of Span 2.
- 3) Because Pire 3 is strong enough and its foundation is so firm that the effect of Span 2’s collapse on it is slight, therefore chain reactions of collapse doesn’t happen. However, under tremendous longitudinal impact of fault, vertical displacement occurred obviously at Span 3.
- 4) There are obvious cracks and displacement on Abutment 5 due to ground motion, and Span 4 collectively moved downwards. Also horizontal shear destruction occurred at the end of arch legs and inclined legs, Span 4 fell to the river bank revetment.

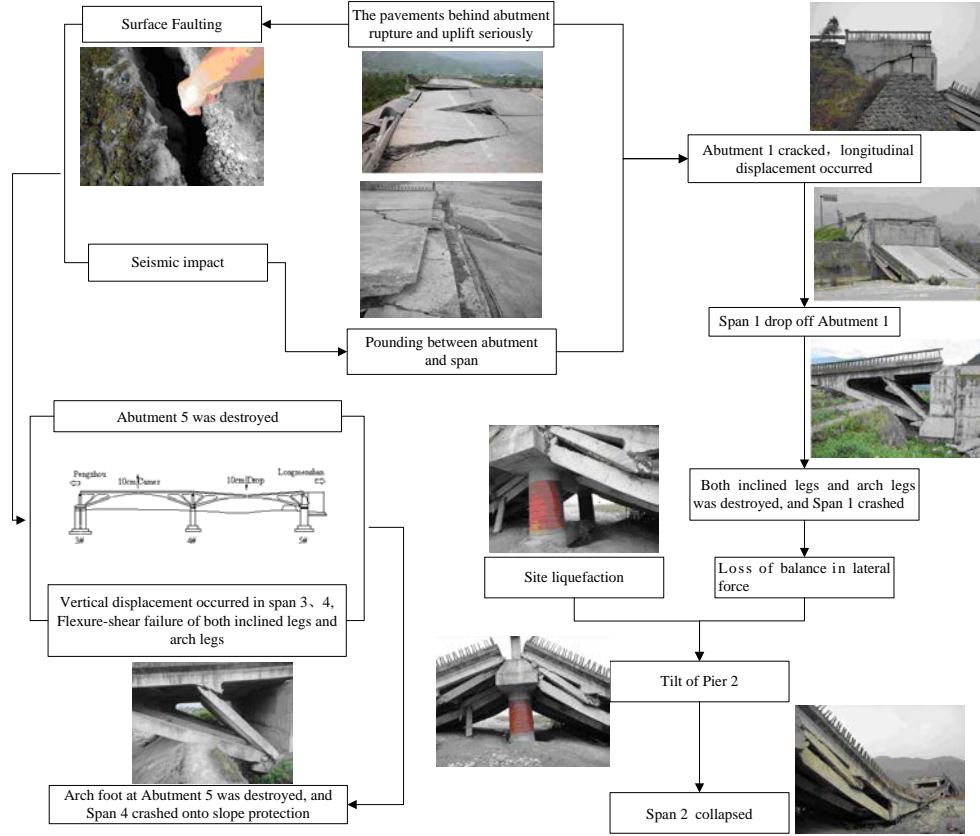


Fig.4 Flow chart of collapse process

3. FIBER ELEMENT WITH AXIAL-SHEAR-FLEXURAL INTERACTION

3.1. Condensation Scheme of Total Strain-Stress Constitution

The condensation scheme is suitable for most engineering applications, such as beam, plate and shell element. Saritas(2009) reported that condensation technique can be extended to consider the presence of transverse reinforcing steel for concrete. Mullapudi(2010) implemented condensation for element stiffness with the Softened Membrane Model. In this paper, the details of condensation process and general formations are presented, and the methodology for fiber beam element with total strain theory is also given. The total strain model adopts a smeared rotating crack approach with refined hysteretic rules defining stress-strain relationship for crack-closing and reopening. For 3D beam element, the stress of reinforced concrete element is given:

$$\begin{aligned} \sigma &= \sigma_c + \sigma_s = \begin{bmatrix} \sigma_{xx}^c & \sigma_{yy}^c & \sigma_{zz}^c & \sigma_{xy}^c & \sigma_{xz}^c & \sigma_{yz}^c \end{bmatrix}^T + \begin{bmatrix} \rho_x f_x & \rho_y f_y & \rho_z f_z & 0 & 0 & 0 \end{bmatrix}^T \\ &= \begin{bmatrix} \sigma_{xx} & 0 & 0 & \sigma_{xy} & \sigma_{xz} & 0 \end{bmatrix}^T \end{aligned} \quad (3.1.1)$$

Where $\sigma_{xx}^c, \sigma_{yy}^c, \sigma_{zz}^c, \sigma_{xy}^c, \sigma_{xz}^c, \sigma_{yz}^c$ are concrete normal and shear stress components in the x, y and z directions respectively, $\rho_x f_x, \rho_y f_y, \rho_z f_z$ are steel stress components.

Strain vectors of concrete and reinforced bar are written as $\varepsilon^c = [\varepsilon_{xx}^c \quad \varepsilon_{yy}^c \quad \varepsilon_{zz}^c \quad \gamma_{xy}^c \quad \gamma_{xz}^c \quad \gamma_{yz}^c]^T$

Assuming $\varepsilon_{xx}^c = \varepsilon_x^s$, $\varepsilon_{yy}^c = \varepsilon_y^s$, $\varepsilon_{zz}^c = \varepsilon_z^s$ total vectors of stress and strain and Jacobian matrix can be written as:

$$\varepsilon = [\hat{\varepsilon} \quad \bar{\varepsilon}]^T, \quad \sigma = [\hat{\sigma} \quad \bar{\sigma}]^T, \quad (\Delta \hat{\sigma} \quad \Delta \bar{\sigma})^T = D^{(n)} (\Delta \hat{\varepsilon} \quad \Delta \bar{\varepsilon})^T \quad (3.1.2)$$

For 2D Timoshenko beam cases, the target stress and strain vectors are:

$$\hat{\sigma} = [\sigma_{xx}^c \quad \sigma_{xy}^c]^T, \quad \hat{\varepsilon} = [\varepsilon_{xx}^c \quad \varepsilon_{xy}^c]^T \quad (3.1.3)$$

In n+1 iteration, corrects the values of strain can be obtained as follows:

$$\hat{\varepsilon}^{(n+1)} = \varepsilon^{(n)} + \Delta \varepsilon^{(n)}, \quad \bar{\varepsilon}^{(n+1)} = \bar{\varepsilon}^{(n)} + \Delta \bar{\varepsilon}^{(n)} \quad (3.1.4)$$

The equilibrium of concrete and steel internal force can be written as

$$\bar{\sigma}^{(n+1)} \approx \bar{\sigma}^{(n)} + D_{21}^{(n)} \Delta \hat{\varepsilon} + D_{22}^{(n)} \Delta \bar{\varepsilon} \rightarrow 0 \quad (3.1.5)$$

So, the condensation of strain can be written as, $\Delta \bar{\varepsilon}^{(n)} = -(\bar{\sigma}^{(n)} + D_{21}^{(n)} \Delta \hat{\varepsilon}) / D_{22}^{(n)}$ (3.1.6)

In n+1 iterations, bring the condensed strain increment to strain:

$$\hat{\varepsilon}^{(n+1)} = \varepsilon^{(n)} + \Delta \varepsilon^{(n)} = \varepsilon^{(n)} - \left(\bar{\sigma}^{(n)} + D_{21}^{(n)} \Delta \bar{\varepsilon}^{(n)} \right) / D_{22}^{(n)} \quad (3.1.7)$$

Calculate the stresses and the tangent operator:

$$\begin{bmatrix} \hat{\sigma}^{(n+1)} \\ \bar{\sigma}^{(n+1)} \end{bmatrix} = D^{(n+1)} \begin{bmatrix} \hat{\varepsilon}^{(n+1)} \\ \bar{\varepsilon}^{(n+1)} \end{bmatrix} = \begin{bmatrix} D_{11}^{(n+1)} & D_{12}^{(n+1)} \\ D_{21}^{(n+1)} & D_{22}^{(n+1)} \end{bmatrix} \begin{bmatrix} \varepsilon^{(n+1)} \\ \bar{\varepsilon}^{(n+1)} \end{bmatrix} \quad (3.1.8)$$

Correcting stress using condensed strain:

$$\Delta \bar{\varepsilon}^{(n+1)c} = \frac{-\bar{\sigma}^{(n+1)}}{D_{22}^{(n+1)}}, \quad \hat{\sigma}^{(n+1)} = \sigma^{(n+1)} + D_{12}^{(n+1)} \Delta \bar{\varepsilon}^{(n+1)c} = \sigma^{(n+1)} - \frac{D_{12}^{(n+1)} \sigma_{zz}^{(n+1)}}{D_{22}^{(n+1)}} \quad (3.1.9)$$

Compute the final tangent operator:

$$\hat{D}^{(n+1)} = \frac{\delta \hat{\sigma}^{(n+1)}}{\delta \hat{\varepsilon}^{(n+1)}} = \frac{\partial \sigma^{(n+1)}}{\partial \varepsilon^{(n+1)}} + \frac{\partial \sigma^{(n+1)}}{\partial \bar{\varepsilon}^{(n+1)}} \frac{\partial \bar{\varepsilon}^{(n+1)}}{\partial \varepsilon^{(n+1)}} = D_{11}^{(n+1)} - \frac{D_{12}^{(n+1)} D_{21}^{(n+1)}}{D_{22}^{(n+1)}} \quad (3.1.10)$$

Where $\frac{\delta \hat{\sigma}^{(n+1)}}{\delta \hat{\varepsilon}^{(n+1)}} = \frac{\delta \sigma^{(n+1)}}{\delta \varepsilon^{(n+1)}} - \frac{D_{12}^{(n+1)}}{D_{22}^{(n+1)}} \frac{\delta \sigma_{zz}^{(n+1)}}{\delta \varepsilon^{(n+1)}}$, $\frac{\delta \bar{\sigma}^{(n+1)}}{\delta \hat{\varepsilon}^{(n+1)}} = \frac{\partial \bar{\sigma}^{(n+1)}}{\partial \varepsilon^{(n+1)}} + \frac{\partial \bar{\sigma}^{(n+1)}}{\partial \bar{\varepsilon}^{(n+1)}} \frac{\partial \bar{\varepsilon}^{(n+1)}}{\partial \varepsilon^{(n+1)}} = D_{21}^{(n+1)} - \frac{D_{22}^{(n+1)} D_{21}^{(n+1)}}{D_{22}^{(n+1)}}$

$$\frac{\delta \hat{\sigma}^{(n+1)}}{\delta \hat{\varepsilon}^{(n+1)}} = D_{11}^{(n+1)} - \frac{D_{12}^{(n+1)} D_{21}^{(n+1)}}{D_{22}^{(n+1)}} - \frac{D_{12}^{(n+1)}}{D_{22}^{(n+1)}} \left(D_{21}^{(n+1)} - \frac{D_{22}^{(n+1)} D_{21}^{(n+1)}}{D_{22}^{(n+1)}} \right)$$

3.2. Element Formation and Total Strain-based Hysteretic Model

The drawback of traditional concentrated plasticity models is that they separate axial-moment interaction from the element behavior (Scott, 2006). Distributed plasticity beam-column elements are

so accurate that can be utilized to simulate axial-moment-shear interaction based on Gauss quadrature rules. Taking axial-shear-flexure interaction into account, Martinelli (2002) developed a fiber beam-column element model which was applied to evaluate the cyclic response of squat bridge piers. Ranzo and Petrangeli (1998) developed a 2D fiber beam-column element based on flexibility method, in which the axial bending response is modeled by a classical fiber discretisation, while the shear response is represented by a nonlinear truss model in which modified microplane model is applied. Mazars et al. (2006) proposed a 3D beam element with stiffness method in which Timoshenko beam theory is applied. Ceresa (2007) adopted 2D Timoshenko beam-column element with MCFT. In this paper, forced and displacement-based beam elements are developed respectively to couple shear and flexural responses for axial force variation. According to Ceresa's study, displacement-based beam is established and forced-based element model which is developed by Cardinetti (2011) is adopted. After condensation iterations, transverse steel stiffness and stress are merged into concrete equivalent stress and stiffness respectively. And section stiffness and internal forces can be obtained by combining the internal forces and stiffness of concrete and longitudinal steel fibers respectively. It is necessary to assemble section stiffness and force in form of the sum of concrete and longitudinal bar stiffness and forces.

Palermo and Vecchio (2003) proposed a constitutive model for concrete consistent with Modified compression field theory. In this model, all parameters were statistically derived from numerous tests. Mi-Geum So (2008) proposed a total strain-based hysteretic material model of 2D planar reinforced concrete structures based on smeared rotating crack modeling concept. It is an extension of Palermo's cyclic model for reinforced concrete structures, as shown in Fig.5 and Fig.6.

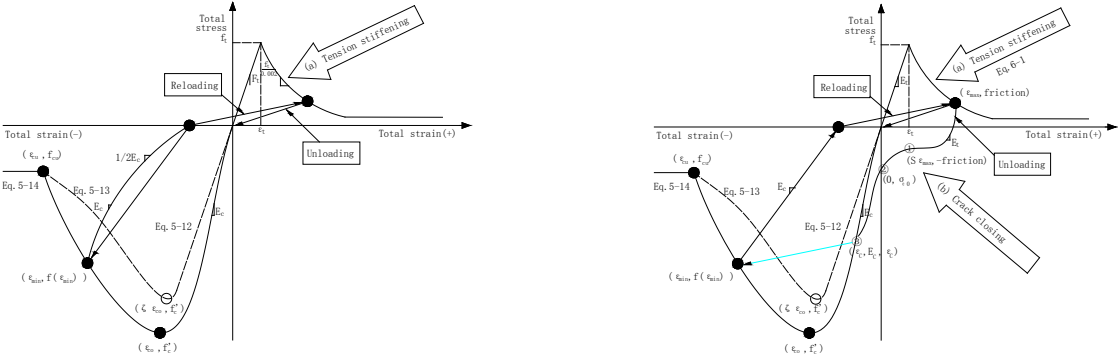


Fig.5 Concrete Model tensile stiffening model. **Fig.6** Concrete Model tensile stiffening model and crack closing model.

3.3. Damage Index

In order to signify damage state, it is necessary to introduce damage indexes. Laborderie (1992) proposed constitutive law of concrete which is based on the damage mechanics with two damage scalar variables. The model was adapted to the description of the behavior generated by the creation of microscopic cracks (lowering of the stiffness) and bound operation, during cycles, with reclosing. In this paper, simplified damage indexes are utilized, as follow:

$$D1 = 1 - \frac{\varepsilon_{ct}}{\varepsilon} \cdot e^{\alpha \left(1 - \frac{\varepsilon}{\varepsilon_{ct}}\right)} \quad (3.3.1)$$

Where $\alpha = \left(\frac{G_f E_0}{l^* f_{ct}^2} - \frac{1}{2}\right)^{-1} \geq 0$, The tensile damage parameter $D1$ measures the material degradation in tension and varies from 0 to 1. While G_f is the fracture energy, f_{ct} is the tensile strength of concrete and l^* is a “characteristic length”.

$$D2 = \left[1 - \frac{\varepsilon_0}{\varepsilon} (1 - A) - A e^{\left(\frac{\varepsilon_0 - \varepsilon}{\varepsilon_c'}\right)} \right], \text{ if } \varepsilon \leq \varepsilon_c' \quad (3.3.2)$$

$$D2 = \left[1 - \frac{B}{\varepsilon} - C e^{\left(\frac{\varepsilon_0 - \varepsilon}{\varepsilon_c'}\right)} \right], \text{ if } \varepsilon > \varepsilon_c' \quad (3.3.3)$$

Where $A = (f_c' - \varepsilon_0 E_0) E_0 / \left[\varepsilon_c' e^{\left(\frac{\varepsilon_0 - 1}{\varepsilon_c'}\right)} - \varepsilon_0 \right]$, The compression damage parameter $D2$ represents the

material degradation in compression, ε_0 is the strain at the elastic limit of concrete in compression. ε_c' is the coordinates at the peak of the stress-stain curve, E_0 is initial elastic modulus of concrete,

$$B = \frac{f_{op} \varepsilon_c' e^{\left(\frac{\varepsilon_0 - 1}{\varepsilon_c'}\right)} - \varepsilon_{op} f_c' e^{\frac{\varepsilon_0}{\varepsilon_c'} \left(1 - \frac{\varepsilon_u}{\varepsilon_0}\right)}}{E_0 \left[\varepsilon_c' e^{\left(\frac{\varepsilon_0 - 1}{\varepsilon_c'}\right)} - \varepsilon_{op} e^{\frac{\varepsilon_0}{\varepsilon_c'} \left(1 - \frac{\varepsilon_u}{\varepsilon_0}\right)} \right]} \text{ and } C = \frac{f_c' - f_{op}}{E_0 \left[\varepsilon_c' e^{\left(\frac{\varepsilon_0 - 1}{\varepsilon_c'}\right)} - \varepsilon_{op} e^{\frac{\varepsilon_0}{\varepsilon_c'} \left(1 - \frac{\varepsilon_u}{\varepsilon_0}\right)} \right]}.$$

4. SEISMIC COLLAPSE ANALYSIS FOR XIAOYUDONG BRIDGE WITH IDA

Incremental Dynamic Analysis (Vamvatsikos, 2002) is an extremely powerful tool for investigating the performance of structures subjected to earthquake ground motions. It involves subjecting a structural model to one(or more) ground motion record(s), each scaled to multiple levels of intensity. Chosen 20 ground motions with different frequency spectrum content for Incremental Dynamic Analysis in Table 3, each record is scaled from 0.1g to 0.8g. The set of ground motions is composed of 19 records recommended by Vamvatsikos (2001) and one ground motion record in Wenchuan Earthquake (Location: CD2-EW, Data Source: CENC).

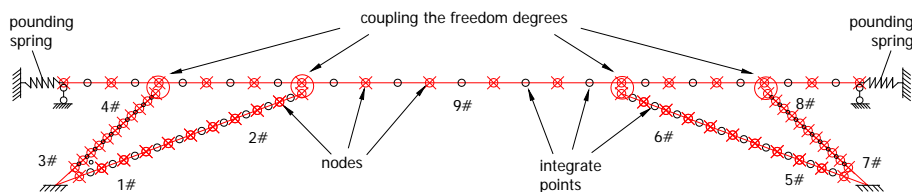


Fig.7 Finite element model with displacement-based element(one integrate point)

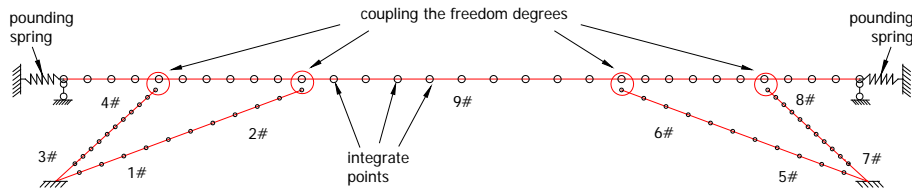


Fig.8 Finite element model with force-based element(three integrate points)

Two kinds of fiber element model are implemented as user elements in ANSYS. There is one integrate point in each displacement-based beam element, and placed three integrate points in each force-based beam element. Using the user elements, the models for Span 1 are established, in which all sections are divided into 12 concrete stripes and 6 longitudinal reinforcing bars, as shown in Fig.7 and Fig.8.

The strain and stress results of transverse reinforcing bars are calculated and recorded on each integrate point. 320 nonlinear time-history analysis was performed totally. Fig.9 and Fig.10 show the mean values of damage indexes max on No.1 section and No.3 section. It should be noted that d1 index (tension damage) is always larger than d2 index (compression damage). It means that structure is prone to shear damage and tension damage. Additionally, comparing damage index maximum of the concrete stripes in No.1 section and No.3 section, component with No.3 section is more fragile in seismic impact. Because of difference in element shape functions and integrated formulations, displacement-based element is more stiff that each damage index is larger than forced element. It is found that convergent results are hard to obtain in displacement-based element models at 0.8g. The stress status of longitudinal and transverse reinforcing bar on three sections are given in Tab.1, when PGA is 0.6g. Moreover, it is shown that the results are compatible with actual damage, in consistence with the investigation and speculation.

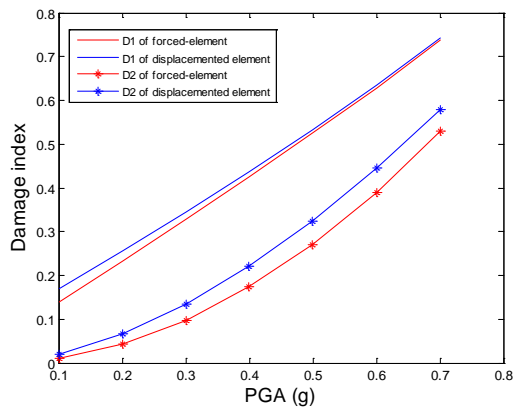


Fig.9 Damage indexes result of No.1 section

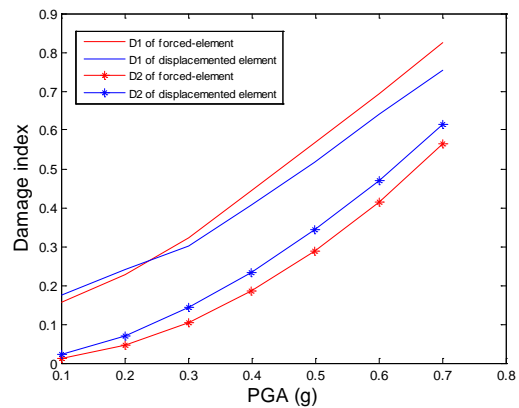


Fig.10 Damage indexes result of No.3 section

Table 1. The status of longitudinal and transverse reinforcing bar at PGA=0.6g
(e for elastic, y for yielding)

NO.groun d motion	element	NO.1 sectio n		NO.3 sectio n		NO.9 sectio n L	NO.groun d motion	element	NO.1 sectio n		NO.3 sectio n		NO.9 sectio n L
		L	T	L	T				L	T	L	T	
1	forced	y	e	y	e	y	11	forced	y	e	y	y	y
	displacement ed	y	e	y	e	y		displacement ed	y	y	y	y	y
2	forced	y	e	y	e	y	12	forced	e	y	e	y	y
	displacement ed	y	e	y	y	y		displacement ed	e	y	e	y	y
3	forced	y	e	y	e	y	13	forced	e	e	e	e	y
	displacement ed	e	e	y	y	y		displacement ed	y	y	y	y	y
4	forced	e	e	y	e	y	14	forced	e	e	e	e	y
	displacement ed	y	e	y	y	y		displacement ed	y	y	y	y	y
5	forced	e	e	e	e	y	15	forced	e	e	e	e	y
	displacement ed	e	y	e	y	y		displacement ed	y	e	e	y	y
6	forced	y	e	y	e	y	16	forced	e	y	e	y	y
	displacement ed	e	y	y	y	y		displacement ed	y	y	e	y	y
7	forced	e	e	y	e	y	17	forced	e	e	e	y	y
	displacement ed	y	e	y	y	y		displacement ed	y	e	e	y	y
8	forced	y	e	e	e	y	18	forced	e	e	e	e	y
	displacement ed	y	y	y	y	y		displacement ed	e	e	y	y	y
9	forced	e	e	y	y	y	19	forced	e	e	e	e	y
	displacement ed	y	y	y	y	y		displacement ed	y	y	y	y	y
10	forced	y	e	y	e	y	20	forced	e	e	e	y	y
	displacement ed	e	e	e	y	y		displacement ed	e	y	e	y	y

5. CONCLUSION

This study was conducted with the aim of capturing the collapse process and mechanisms of failure of Xiaoyudong Bridge. Based on post-earthquake damage assessment and site fault investigation, collapse process can be speculated and the conclusion is made that the bottoms of inclined legs was

the vulnerable component subjected to seismic load. According to damage survey, there are extensive shear cracks and flexural cracks occurred to the bottom of inclined legs. Two kinds of beam element models were implemented as a user element into ANSYS. To highlight the development of damage, two damage indexes were chosen. With performing IDA, the speculation which was deduced by post-earthquake investigation is identified.

ACKNOWLEDGMENTS

This research is supported by the National Science Foundation of China (No.50978221).

REFERENCES

- Ceresa P., Petrini L., Pinho R. (2007), Flexure-shear Fiber Beam-Column Elements for Modelling Frame Structures under Seismic Loading – State of the art,” *Journal of Earthquake Engineering*, Vol.11, Supplement 1, pp. 46-88.
- Filippo Cardinetti Fiber beam-columns models with flexure-shear interaction for nonlinear analysis of reinforced concrete structures doctoral thesis 2011, universita di bologna
- Kawashima, K., Takahashi, Y., Ge, H., Wu, Z., and Zhang, J. (2009), Reconnaissance Report on Damage of Bridges in 2008 Wenchuan, China, Earthquake, *Journal of Earthquake Engineering*, Vol.13, pp. 965-996.
- Martinelli, L. (1998-2002) ,Modellazione di Pile da Ponte in C.A. a travata soggetti ad ecitazione sismica, Phd. thesis, Dipartimento di Ingegneria Strutturale, Politecnico di Milano, Milano, Italy Ranzo and Petrangeli (1998)
- Mazars, J. Kotronis, P., Ragueneu, F. e Casaux, G. et al. (2006). Using Multifiber Beams to Account for Shear and Torsion. Application to Concrete Structural Element, *Computer Methods in Applied Mechanics and Engineering* 195(52), 7264-7281.
- Mullapudi, Ravi, Ashraf Ayoub, (2010) ,Modeling of the seismic behavior of shear-critical reinforced concrete columns, *engineering structures*, 32, 2010, 3601-3615
- Palermo, D. and Vecchio, F. J. (2007), Simulation of Cyclically Loaded Concrete Structures Based on the Finite-Element Method,” *Journal of Structural Engineering*, ASCE, V.133, No. 5, May 2007, pp. 728-738.
- Ren, H., Li, W., Zhang, J. and Chen, H.: Inspection and Design Suggestion on Rigid-Frame Arch Bridge, the 1st Chinese-Croatian Joint Colloquium on Long Arch Bridge, pp. 309-315, 2008
- Saritas A, Filippou FC. (2009), Inelastic axial-flexure–shear coupling in a mixed formulation beam finite element. *International Journal of Non-Linear Mechanics*; 44: 913-922.
- Scott, M.H. and G.L. Fenves. Plastic Hinge Integration Methods for Force-Based Beam-Column Elements. *Journal of Structural Engineering*, 132(2):244-252, February 2006.
- Vamvatsikos D, Cornell CA. (2001) ,Tracing and post-processing of IDA curves: Theory and software implementation. Report No. RMS-44, RMS Program, Stanford University, Stanford, 2001.